Biochemical and Biophysical Research Communications 443 (2014) 370–375

Contents lists available at ScienceDirect

Biochemical and Biophysical Research Communications

journal homepage: www.elsevier.com/locate/ybbrc

Solution structure of CEH-37 homeodomain of the nematode *Caenorhabditis elegans*

Sunjin Moon [a], Yong Woo Lee [b], Woo Taek Kim [b], Weontae Lee [a,*]

[a] Structural Biochemistry and Molecular Biophysics Lab, Department of Biochemistry, College of Life Science and Biotechnology, Yonsei University, Seoul 120-749, Republic of Korea
[b] Department of Systems Biology, College of Life Science and Biotechnology, Yonsei University, Seoul 120-749, Republic of Korea

ARTICLE INFO

Article history:
Received 12 November 2013
Available online 19 December 2013

Keywords:
Solution structure
NMR spectroscopy
Nematode *Caenorhabditis elegans*
CEH-37
Telomere-binding protein
Homeodomain

ABSTRACT

The nematode *Caenorhabditis elegans* protein CEH-37 belongs to the paired OTD/OTX family of homeobox-containing homeodomain proteins. CEH-37 shares sequence similarity with homeodomain proteins, although it specifically binds to double-stranded *C. elegans* telomeric DNA, which is unusual to homeodomain proteins. Here, we report the solution structure of CEH-37 homeodomain and molecular interaction with double-stranded *C. elegans* telomeric DNA using nuclear magnetic resonance (NMR) spectroscopy. NMR structure shows that CEH-37 homeodomain is composed of a flexible N-terminal region and three α-helices with a helix-turn-helix (HTH) DNA binding motif. Data from size-exclusion chromatography and fluorescence spectroscopy reveal that CEH-37 homeodomain interacts strongly with double-stranded *C. elegans* telomeric DNA. NMR titration experiments identified residues responsible for specific binding to nematode double-stranded telomeric DNA. These results suggest that *C. elegans* homeodomain protein, CEH-37 could play an important role in telomere function via DNA binding.

1. Introduction

Members of the well-conserved OTD/OTX family of homeodomain (HD) proteins have been implicated in the development and patterning of the central nervous system and sensory structures in multiple species [1–3]. The nematode *Caenorhabditis elegans* CEH-37 protein belongs to the OTD/OTX family of homeobox proteins. CEH-37 is transiently expressed in AWB olfactory neurons and it is required for their development. Functional studies suggest that embryonic expression of *CEH-37* in AWB neurons is sufficient to trigger the expression of *lim-4*, which maintains its expression via auto-regulation [1]. Previous report suggests that CEH-37 functions as a telomere-binding protein in *C. elegans* and it is primarily co-localized at chromosome ends *in vivo* [4]. CEH-37 is also required for chromosome stability *in vivo* together with *mrt-2*, which is a checkpoint-protein gene. *CEH-37* encodes a protein that is 278 amino acids long and contains a homeodomain motif in the N-terminal region. Typically, the HD consists of 60 highly conserved residues and forms an N-terminal arm and a third helix, which recognizes specific DNA sequences that bear a TAAT core [5–8]. Consistent with this, CEH-37 specifically binds double-stranded *C. elegans* telomeric DNA with TTAGGC repeats, which is different from that of other eukaryotic species [4].

It has been proposed that the CEH-37 HD could play an important role as a Myb-like domain of telomere-binding protein although CEH-37 has low sequence identity with that of other OTX-related proteins. Therefore, it is of essence to know the structure and molecular interaction with telomeric DNA of CEH-37 in understating the molecular mechanism, which underlies its biological function as a transcriptional activator and telomere-binding protein. Here, we present the high-resolution solution structure of the CEH-37 HD by nuclear magnetic resonance (NMR) spectroscopy. In addition, we determined the detailed molecular interactions between CEH-37 HD and double-stranded *C. elegans* telomeric DNA by data from NMR titration, steady state XNOE, and fluorescence experiments. Our data provide strong evidence that CEH-37 HD binds specifically to the *C. elegans* double-stranded telomeric DNA although CEH-37 is a homeodomain protein [9–11].

2. Materials and methods

2.1. Cloning, protein purification, and sample preparation

The cDNA fragment encoding the *C. elegans* CEH-37 HD comprising residue from Pro38 to Pro104 was amplified by PCR. The amplified cDNA fragment was subcloned into the *Bam*HI and *Xho*I sites of the modified expression vector pET32a (Novagen)

Abbreviations: NMR, nuclear magnetic resonance; TBP, telomere-binding protein; HD, homeodomain; *C. elegans*, *Caenorhabditis elegans*; NOE, nuclear Overhauser effect; HSQC, heteronuclear single quantum coherence.

* Corresponding author. Address: Department of Biochemistry, College of Life Science and Biotechnology, Yonsei University, 50 Yonsei-ro, Seodaemun-gu, Seoul 120-749, Republic of Korea. Fax: +82 2 363 2706.
E-mail address: wlee@spin.yonsei.ac.kr (W. Lee).

0006-291X/$ - see front matter © 2013 Elsevier Inc. All rights reserved.
http://dx.doi.org/10.1016/j.bbrc.2013.11.133

fused with N-terminal hexahistidine affinity tags and TEV cleavage sites. The resultant plasmids were transformed into *Escherichia coli* strain BL21 (DE3). All plasmid DNAs were grown in both LB and M9 minimal media at 37 °C to an $OD_{600} \approx 0.6$. Cells were harvested by centrifugation and stored at −70 °C.

For NMR experiments, CEH-37 HD proteins were labeled with ^{15}N or $^{13}C/^{15}N$ by cultivating in M9 minimal medium containing $^{15}NH_4Cl$ (Cambridge Isotope Laboratories Inc.) and/or U-$^{13}C_6$-glucose (Cambridge Isotope Laboratories Inc.). The labeled proteins were extracted, isolated, and subjected to affinity chromatography. After affinity chromatography, we removed the TRX-His tag (pET32a) by incubation with tobacco etch virus protease for 12 h at 25 °C. The purified proteins were then subjected to size-exclusion chromatography on Superdex 75 (Amersham Biosciences) at the final buffer (10 mM HEPES, pH 7.5, 500 mM NaCl, 2 mM DTT, 0.01% NaN_3).

2.2. NMR experiments and structure determination of CEH-37 HD

All NMR experiments were recorded on Bruker 500 MHz and 800 MHz spectrometers equipped with a *z*-shielded gradient triple-resonance cryoprobe. Three-dimensional NMR data have been served for sequential assignments, which are HNCO, HNCACB, CBCA(CO)NH, HNCA, and HCCH-TOCSY experiments [12–17]. To determine the three-dimensional structure, ^{15}N-edited NOESY (τ_m = 150 ms) and ^{13}C-edited NOESY-HSQC (τ_m = 150 ms) experiments were performed [18–21]. Backbone dihedral angle restraints were derived from Hα, $^{13}C\alpha$, $^{13}C\beta$, and ^{13}CO chemical shifts with the program TALOS. All NMR data were processed using the XWINNMR program and NMRpipe/NMRDraw software. Structure calculations for CEH-37 HD were carried out using CYANA 2.2.5. A total of 100 structures were calculated, and 20 structures with the lowest target-function values were chosen for detailed analysis. A summary of NMR-derived restraints and structural statistics of CEH-37 HD is shown in Table 1. The final structures were retained and validated by the program PROCHECK [22]. Analysis with PROCHECK-NMR shows that more than 99% of residues have backbone dihedral angles in allowed regions of the Ramachandran plot, with 0.1% of residues in disallowed regions. The residues in the generously allowed and the disallowed regions are Asn41 and Arg42, which are located in the N-terminal tail region. Final structures were analyzed and visualized using the programs PyMOL and MOLMOL [23]. The electrostatic surface potential was calculated with the program APBS. NMR chemical shifts were deposited in the Biological Magnetic Resonance Bank (BMRB) under accession code 19600. The atomic coordinates of the final 20 structures and the energy-minimized average structure of CEH-37 HD were deposited in the Protein Data Bank (PDB) under accession code 2mgq. The following servers were used for sequence and structural analyses: BLAST (http://blast.ncbi.nlm.nih.gov/Blast.cgi), DALI (http://ekhidna.biocenter.helsink.fi/dali-server), and SCOP (http://scop.mrc-lmb.cam.ac.uk/scop).

2.3. NMR titration with telomeric DNA and XNOE experiments

NMR titration experiments were performed by recording a series of two-dimensional (2D) ^{15}N-^{1}H HSQC spectra on uniformly ^{15}N-labeled CEH-37 HD (0.5 mM) in the presence of different amounts of double stranded *C. elegans* telomeric DNA ($(TTAGGC)_2$). Samples were prepared in 10 mM HEPES at pH 7.5 containing 100 mM NaCl, 2 mM DTT, and 0.01% NaN_3. Chemical-shift perturbations were calculated using the equation $\Delta\delta_{AV} = [(\Delta\delta_{1H})^2 + (\Delta\delta_{15N}/5)^2]^{1/2}$, where $\Delta\delta_{AV}$, $\Delta\delta_{1H}$, and $\Delta\delta_{15N}$ are the average, proton, and ^{15}N chemical-shift changes, respectively. To investigate the dynamic properties of both free and DNA bound form of CEH-37 HD, the steady-state heteronuclear ^{1}H,^{15}N-NOE (XNOE) was measured [24,25]. The XNOE data were collected for $2048(t_2) \times 128(t_1)$ dimensions with a 3-s recycle delay. Both unsaturated and saturated XNOE spectra were acquired by interleaving pulse sequences, and they were separately processed for analysis. The heteronuclear XNOE values were determined by the ratio of the peak heights produced by the unsaturated versus saturated XNOE spectra, and error values were calculated using the equation $\sigma_{NOE}/NOE = [(\sigma I_{sat}/I_{sat})^2 + (\sigma I_{unsat}/I_{unsat})^2]^{1/2}$, where I_{sat} and I_{unsat} represent the cross-peak intensities, and σI_{sat} and σI_{unsat} represent the root-mean-square noise value of the background in proton-saturated and proton-unsaturated spectra, respectively.

Table 1
NMR structural statistics.

Distant restraints in the structure calculation	
All	1172
Short range {|i − j| = 1}	675
Medium range {$2 \leqslant \|i-j\| \leqslant 5$}	310
Long range {|i − j| > 5}	187
Hydrogen bond restraints[a]	22
Dihedral angle restraints	
All	66
Φ	33
Ψ	33
Residual violations	
CYANA target functions, Å	4.21 ± 0.11
NOE upper distance constrain violation	
Ave, Å (<0.1 A)	0.0191 ± 0.0005
Dihedral angle constrain violations	
Ave,° (<5°)	2.56 ± 0.05
Vander Waals violations	
Ave, Å (<0.2 A)	10.1 ± 0.4
RMS deviations from the average coordinate[b], Å	
Backbone atoms	0.31 ± 0.11
All heavy atoms	1.13 ± 0.12
Ramachandran statistics, % of all residues	
Residues in most favored regions	72.3%
Residues in additional allowed regions	26.5%
Residues in generously allowed regions	1.1%
Residues in disallowed allowed regions	0.1%

[a] Two restraints per one hydrogen bond.
[b] RMSD values for residues 51–102 a.a.

2.4. Fluorescence experiments

Double-stranded oligonucleotides (5′-TTAGGCTTAGGC-3′ and 5′-GCCTAAGCCTAA-3′) were synthesized and purified using polyacrylamide gel electrophoresis (PAGE) (Operon). Binding affinity between *C. elegans* telomeric DNA and CEH-37 HD were measured on a model RF-5301PC spectro-fluorophotometer (Shimadzu, Kyoto, Japan). CEH-37 HD in NMR buffer (10 mM HEPES,100 mM NaCl, 2 mM DTT, and 0.01% NaN_3 at pH 7.5) was titrated to a molar ratio of 1:1 (CEH-37 HD: *C. elegans* telomeric DNA) using a 2 ml thermostat cuvette. Samples were excited at 280 nm, and emission spectra were recorded for light scattering effects from 270 to 500 nm [26]. We calculated the K_d value using the equation $\log(F_0 - F/F) = \log(1/K_d) + n\log[\text{ligand}]$, where F_0 and F represent fluorescence intensity of the protein at 344 nm in the absence and presence of DNA, respectively. The number n represents the ligand binding site of the protein.

3. Results and discussion

3.1. Solution structure of CEH-37 homeodomain

All backbone and side-chain resonances were completely assigned using data from HNCA, CBCACONH, HNCACB, HCCH-TOCSY, and ^{15}N-edited NOESY experiments. The 2D [^{1}H-^{15}N] HSQC

spectrum of CEH-37 HD with assignment showed that most of the backbone NH resonances are spread uniformly over the spectrum, indicative of well-folded protein (Fig. 1A). The summary of sequential and nuclear Overhauser effect (NOE) connectivity is shown in Fig. 1B. The NOE patterns clearly indicate that CEH-37 HD contains three α-helical regions and two connecting loops, similar to those found in other HD proteins. Secondary structures were also confirmed by data from the chemical shift indices (CSI) and $^{3}J_{HN}\alpha$ coupling constants (Fig. 1B). A total of 1172 unambiguous NOEs (675 short-range ($|i-j|=1$), 310 medium-range ($1<|i-j|<5$), 187 long-range ($|i-j|\geqslant 5$) NOE constraints), 22 backbone hydrogen bonds, and 66 dihedral angle restraints from NMR experiments

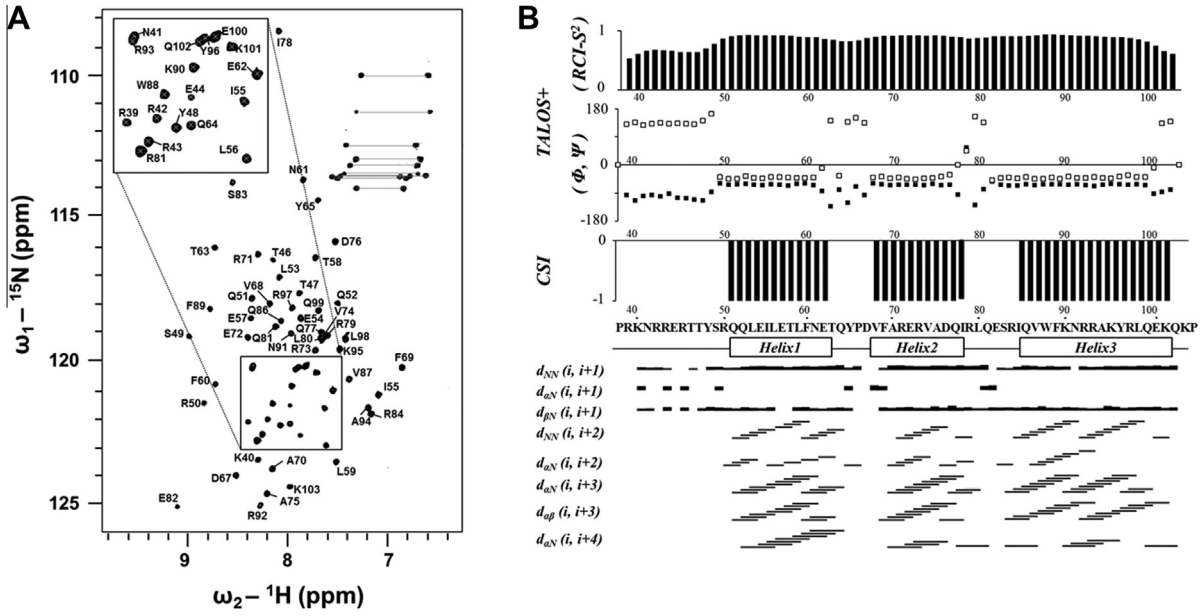

Fig. 1. Two-dimensional HSQC spectrum and secondary structural elements of CEH-37 HD. (A) ^{1}H-^{15}N HSQC spectrum of CEH-37 HD with resonance assignments. The spectrum was collected at pH 7.5 using a Bruker 800 MHz spectrometer. (B) Summary of NMR data. The NOE connectivities were summarized by the line thickness classified by NOE intensity. NOEs were extracted from ^{15}N-edited NOESY and ^{13}C-edited NOESY spectra. The amino acid sequence for of CEH-37 HD is shown, and the helical regions correspond with TALOS and chemical shift index values. Phi (Φ) and psi (Ψ) values indicate backbone dihedral angles of the CEH-37 HD, which were calculated using TALOS+. Secondary structure (SS) values from TALOS + suggest α-helices. Predicted secondary structures of CEH-37 HD are drawn on the bottom with the sequence.

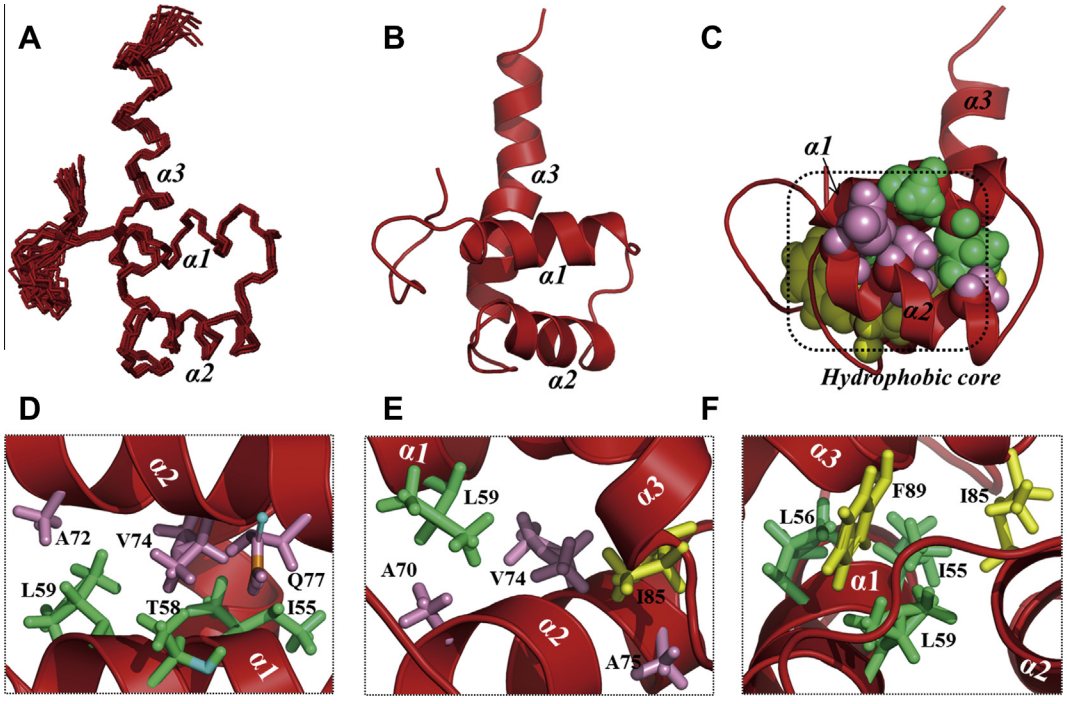

Fig. 2. Solution structure of CEH-37 HD. (A) Superposition of the backbone traces from the final ensemble of 20 solution structures of CEH-37 HD. The structures are shown by superimposing residues 38–104 (in red). (B) Ribbon representation of the lowest energy conformer of CEH-37 HD. (C) Hydrophobic core that contributes to stabilizing the overall folding of the three helices. (D–F) Close-upviews of the hydrophobic core formed by the side-chains of residues between helix 1 and helix 2, between helix 2 and helix 3, and between helix 1 and helix 3. (For interpretation of the references to color in this figure legend, the reader is referred to the web version of this article.)

were derived for structure calculation. The statistics of the experimental constraints and structural quality of CEH-37 HD are summarized in Table 1. The 20 lowest target-function structures have an average root-mean-square deviation (RMSD) of 0.31 ± 0.11 Å for backbone atoms and a RMSD value of 1.13 ± 0.12 Å for all heavy atoms in the structural region (Fig. 2A).

The overall structure of CEH-37 HD forms a globular structure very similar to that of other HDs, which contains an extended N-terminal arm (residues 38–50) and three α-helices (α-helix 1 (residues 51–62), α-helix 2 (residues 67–78), and α-helix 3 (residues 85–102)) connected by loops (Fig. 2B). Two helices, α1 and α2 have similar lengths and α3 is longer than others. Helices α1 and α2 pack against each other in an antiparallel arrangement. Helix α3 is approximately perpendicular to the two helices, and the hydrophobic patch of the three α-helices stabilizes the structure of CEH-37 HD (Fig. 2C).

The hydrophobic interaction is a major driving force for three helices (hydrophobic patch 1 between helices α1 and α2 (Fig. 2D), hydrophobic patch 2 between helices α2 and α3 (Fig. 2E), and hydrophobic patch 3 between helices α1 and α3 (Fig. 2F)). The hydrophobic residues involved for helix packing are Ile55, Leu56, Thr58, Leu59, Ala70, Val74, Ala75, Qln77, Ile85, and Phe89. The solution structure of CEH-37 HD consists of a flexible N-terminal arm and three α-helices with helix-turn-helix motif, which is a typical HD fold of homeodomain proteins [9].

3.2. Telomeric DNA binding of CEH-37 HD by NMR titration

Although most homeodomains recognize similar DNA sequence with TAAT motif, it has been shown that CEH-37 HD specifically binds double-stranded *C. elegans* telomeric DNA with TTAGGC sequence [4]. Data from size-exclusion chromatography shows that CEH-37 HD forms a binary complex with double-stranded *C. elegans* telomeric DNA (Fig. 3A). The molecular weight of CEH-37 HD (8.4 kDa) and telomeric DNA (7.9 kDa) complex was determined as 16 kDa, showing that two molecules form a 1:1 complex. Data from SDS–PAGE and agarose gel electrophoresis confirmed formation of the binary complex of CEH-37 HD and telomeric DNA. Fluorescence experiment shows that CEH-37 HD interacts strongly with telomeric DNA and dissociation constant (K_d) was determined to be 0.74 ± 0.02 μM (Fig. 3B).

To identify the residues important for interaction with *C. elegans* telomeric DNA, we analyzed the chemical-shift perturbation upon DNA binding by 2D-HSQC titration experiments (Fig. 3C). When telomeric DNA was added into CEH-37 HD, large chemical-shift changes were observed for residues in the both N-terminal

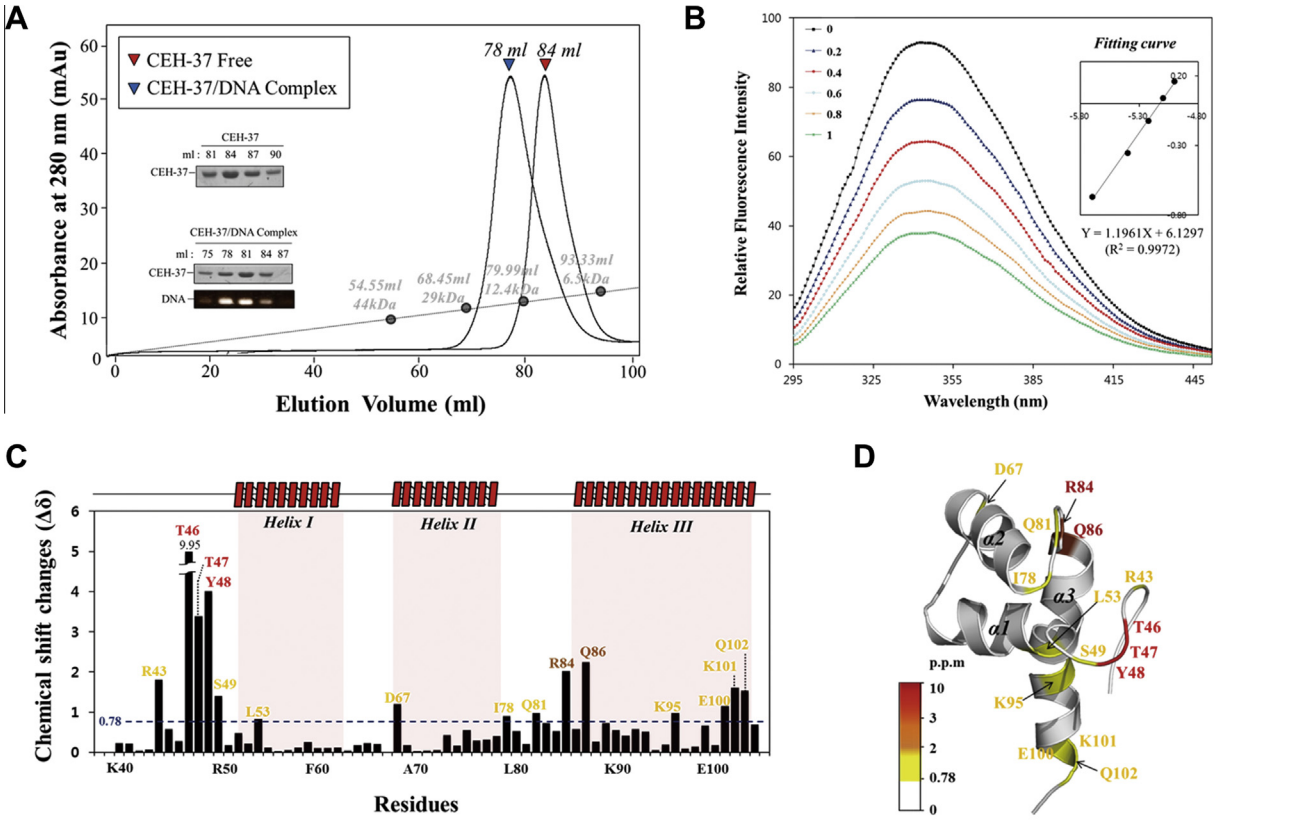

Fig. 3. Characterization of CEH-37 HD binding to double-stranded *C. elegans* telomeric DNA. (A) Interaction of CEH-37 HD with double-stranded *C. elegans* telomeric DNA in a size-exclusion assay. The molecular weight marker proteins used were ovalbumin (44 kDa), carbonic anhydrase (29 kDa), ribonuclease A (12.4 kDa), and a protinin (6.5 kDa). The estimated elution positions for the CEH-37 HD/double-stranded *C. elegans* telomeric DNA complex and for CEH-37 HD are indicated by blue and red arrows, respectively (blue arrow, CEH-37 HD/double-stranded *C. elegans* telomeric DNA complex; red arrow, CEH-37 HD). SDS–PAGE and agarose gel electrophoresis were used to show protein and double-stranded *C. elegans* telomeric DNA contents of the peaks, respectively. The molecular weights of free protein and protein–DNA complex were calculated using the following equation: $\log Y = -1.2177X + 6.263$, where $R^2 = 0.9942$, and $X = V_e/V_o$ (V_o = 45.85 ml, V_e = elution volume, $Y = \log M_W$). (B) Fluorescence spectra with a fitting plot of CEH-37 HD in the presence of difference mixing ratios of double-stranded DNA [1:0 (black), 1:0.2 (blue), 1:0.4 (red), 1:0.6 (cyan), 1:0.8(orange), 1:1 (green)] at pH 7.5. (C) Chemical-shift difference (CSD) analysis for interaction-site mapping of the CEH-37 HD/double-stranded *C. elegans* telomeric DNA complex using NMR titration. ^{15}N-labeled CEH-37 HD was titrated with double-stranded *C. elegans* telomeric DNA in a 1:1 molar ratio. The average chemical-shift changes were calculated using the following formula: $\Delta\delta_{total} = [(\Delta\delta H^N)^2 + (\Delta\delta N^H)^2]^{1/2}$. The residues that displayed chemical shifts greater than 0.78 were labeled and classified with respect to the chemical shift change ($\triangle\delta$ value). Yellow, 0.78 < $\triangle\delta$ < 2; brown, 2 < $\triangle\delta$ < 3; red, 3 < $\triangle\delta$. (D) Ribbon presentation of the DNA-binding site of CEH-37 HD indicating the DNA-binding residues that exhibit chemical shift changes. Yellow, 0.78 < $\triangle\delta$ < 2; brown, 2 < $\triangle\delta$ < 3; red, 3 < $\triangle\delta$. (For interpretation of the references to color in this figure legend, the reader is referred to the web version of this article.)

region (R43, T46, T47 and Y48), a α2–α3 loop (I78, Q81 and R84) and α3 (Q86, E100, K101 and Q102) (Fig. 3D). The residues that did not show noticeable chemical shift changes upon DNA binding are mainly located on the α-helix regions except helix 3, suggesting that the chemical shift perturbations are due to DNA interaction. This implies that both N-terminal region and HTH motif of CEH-37 HD play an important role in binding of *C. elegans* telomeric DNA.

3.3. Heteronuclear NOE and DNA binding

The ^{15}N-^{1}H heteronuclear NOEs for structural regions were observed as 0.7–1.0 and XNOE values show that the secondary structural regions of CEH-37 HD are relatively rigid (Fig. 4A). N-terminal region of CEH-37 HD becomes more rigid upon DNA binding than that of the free protein, implying that the N-terminal region involves in binding of double-stranded *C. elegans* telomeric DNA. Interestingly, α1 region of CEH-37 HD/DNA complex exhibits bigger steady-state heteronuclear NOEs than those of the free form, suggesting that α1 also becomes rigid upon DNA binding. The CEH-37 HD/telomeric DNA complex structure generated by HADDOCK modeling revealed that the overall conformation and the helix orientations of CEH-37 HD upon DNA binding were very similar to that of known TBP/DNA complexes (Fig. 4B). CEH-37 HD interacts with the major groove indouble-stranded *C. elegans* telomeric DNA through helix 2 and helix3 composed of the positively charged surfaces. Highly conserved residues R43, T46, T47 and Y48 in the N-terminal region interact most closely with the nucleotides in telomeric DNA.

3.4. Structural comparison of CEH-37 HD with other homeodomain proteins

Homeodomain proteins are a superfamily of transcription factors that were first identified in a number of *Drosophila* homeotic and segmentation proteins. The homeobox genes can be subdivided into classes, including LIM, POU, HNF, CUT, OTX, and TALE [2,5,6]. CEH-37 is predicted to encode a member of the OTX family of HD proteins [3,4]. Data from multiple-sequence alignment show that the primary sequence of CEH-37 HD is well conserved among known HD proteins, such as that from human (PDB: 2DMU, 2L7M, 3CMY), mouse (PDB: 2DMS), and *Drosophila* (PDB: 3A02, 1FJL) (Fig. 4C). Sequence homology is approximately 66–69% and backbone RMSDs among homeodomains are calculated as 2.7–2.9 Å. The mouse OTX2 HD has the highest Z-score with 69% sequence identity and backbone RMSD of 2.7 Å compared with those of CEH-37 HD.

3.5. Functional implication of CEH-37 HD

In nematode cells, *CEH-37* was identified as a homeobox family member and it encodes a 278-amino acid protein containing a HD (67 amino acids) in the N-terminal region. Previous reports suggested that CEH-37 could function as a telomere-binding protein although it is a homeodomain protein [1,4]. In this study, we present the solution structure and DNA binding mode of CEH-37 HD, which is the first three-dimensional structure and telomeric DNA interaction of the *C. elegans* HD-containing protein. Although CEH-37 HD has low sequence similarity with that of the Myb-like domain proteins, the global fold and DNA interaction mode of CEH-37 HD is similar to that of the Myb-like domain of telomere-binding proteins [4–6,10]. These results could be explainable by the hypothesis of distinct evolution of homeodomain proteins as transcription factors and as well as telomere-binding proteins, such as TBPs with Myb-like domains. In fact, the Myb-like motif has been recruited frequently from ancestral forms of the transcription factors [27–29]. NMR structure and DNA binding of CEH-37 HD as a *C. elegans* telomere-binding protein suggest that TBPs might be evolutionarily conserved in terms of structural homology rather than sequence homology.

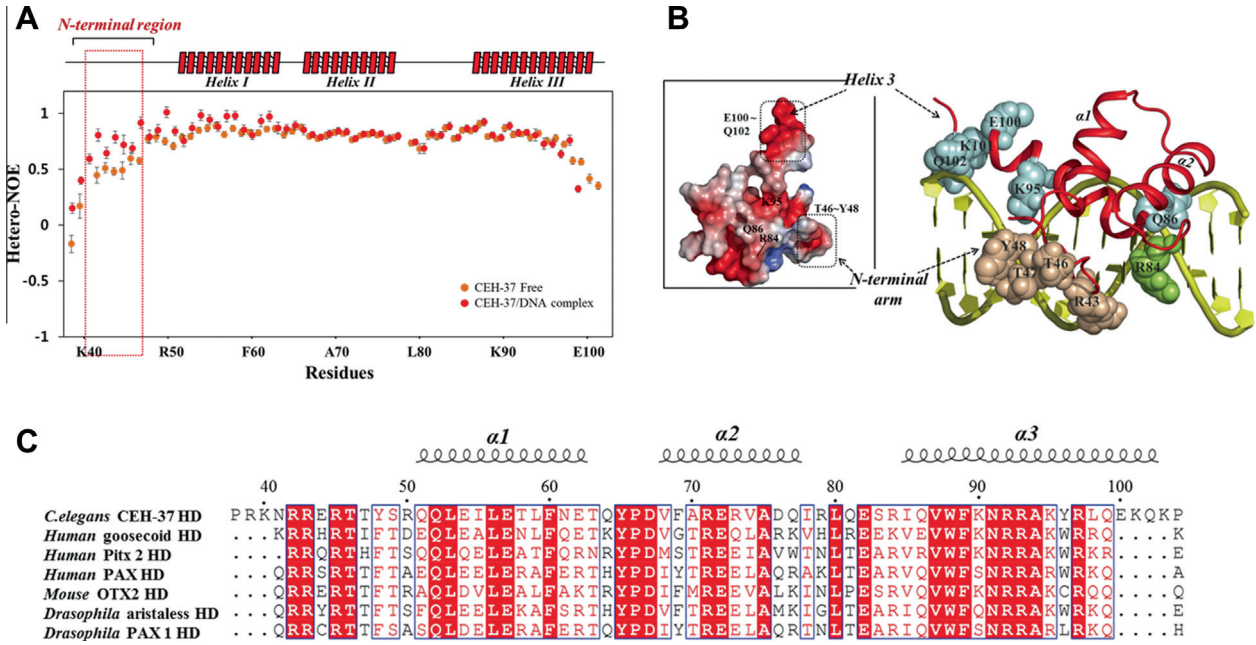

Fig. 4. Heteronuclear NOE plot and multiple sequence alignment of homeodomain proteins. (A) Backbone dynamics profile of both free CEH-37 HD and DNA bound form. Heteronuclear NOEs (XNOEs) were plotted for each residue and the corresponding secondary structure (depicted above the panel). (B) The electrostatic potential surface (blue, positively charged; red, negatively charged; white, neutral residues) of CEH-37 HD calculated with the APBS program and a structure model of the CEH-37 HD/DNA complex based on data from NMR data. Spherical presentation is used for resides involved in DNA-binding. (C) Multiple-sequence alignment of CEH-37 HD with homeodomain family proteins from other species. Sequence alignment was performed using T-Coffee software and rendered further using Esprit software. (For interpretation of the references to color in this figure legend, the reader is referred to the web version of this article.)

Acknowledgments

This work was supported by the Basic Science Research Program (NRF-2012R1A1A0242120) through the National Research Foundation of Korea (NRF) funded by the Ministry of Education, Science and Technology.

References

[1] A. Lanjuin, M.K. VanHoven, C.I. Bargmann, J.K. Thompson, P. Sengupta, Otx/otd homeobox genes specify distinct sensory neuron identities in *C. elegans*, Dev. Cell 5 (2003) 621–633.
[2] D. Acampora, M. Gulisano, A. Simeone, Genetic and molecular roles of Otx homeodomain proteins in head development, Gene 246 (2000) 23–35.
[3] A. Simeone, Otx1 and Otx2 in the development and evolution of the mammalian brain, EMBO J. 17 (1998) 6790–6798.
[4] S.H. Kim, S.B. Hwang, I.K. Chung, J. Lee, Sequence-specific binding to telomeric DNA by CEH-37, a homeodomain protein in the nematode *Caenorhabditis elegans*, J. Biol. Chem. 278 (2003) 28038–28044.
[5] C.O. Pabo, R.T. Sauer, Transcription factors: structural families and principles of DNA recognition, Annu. Rev. Biochem. 61 (1992) 1053–1095.
[6] S. Banerjee-Basu, A.D. Baxevanis, Molecular evolution of the homeodomain family of transcription factors, Nucleic Acids Res. 29 (2001) 3258–3269.
[7] D.S. Wilson, B. Guenther, C. Desplan, J. Kuriyan, High resolution crystal structure of a paired (Pax) class cooperative homeodomain dimer on DNA, Cell 82 (1995) 709–719.
[8] K. Miyazono, Y. Zhi, Y. Takamura, K. Nagata, K. Saigo, T. Kojima, M. Tanokura, Cooperative DNA-binding and sequence-recognition mechanism of aristaless and clawless, EMBO J. 29 (2010) 1613–1623.
[9] K. Ogata, S. Morikawa, H. Nakamura, A. Sekikawa, T. Inoue, H. Kanai, A. Sarai, S. Ishii, Y. Nishimura, Solution structure of a specific DNA complex of the Myb DNA-binding domain with cooperative recognition helices, Cell 79 (1994) 639–648.
[10] T. Nishikawa, A. Nagadoi, S. Yoshimura, S. Aimoto, Y. Nishimura, Solution structure of the DNA-binding domain of human telomeric protein, hTRF1, Structure (1998) 1057–1065.
[11] M.J. Giraud-Panis, S. Pisano, A. Poulet, M.H. Le Du, E. Gilson, Structural identity of telomeric complexes, FEBS Lett. 584 (2010) 3785–3799.
[12] G.W. Vuister, A. Bax, Quantitative J correlation: a new approach for measuring homonuclear three bond J(HNHa) coupling constants in 15N-enriched proteins, J. Am. Chem. Soc. 115 (1993) 7772–7777.
[13] S. Grzesiek, A. Bax, Improved 3D Triple-resonance NMR techniques applied to a 31-kDa protein, J. Magn. Reson. 96 (1992) 432–440.
[14] J. Stonehouse, R.T. Clowes, G.L. Shaw, J. Keeler, E.D. Laue, Minimisation of sensitivity losses due to the use of gradient pulses in triple-resonance NMR of proteins, J. Biomol. NMR 5 (1995) 226–232.
[15] D.R. Muhandiram, L.E. Kay, Gradient-enhanced triple-resonance three dimensional NMR experiments with improved sensitivity, J. Magn. Reson. 103 (1994) 203–216.
[16] M. Ikura, L.E. Kay, A. Bax, A novel approach for sequential assignment of 1H, 13C, and 15N spectra of proteins: heteronuclear triple-resonance three dimensional NMR spectroscopy application to calmodulin, Biochemistry 29 (1990) 4659–4667.
[17] A. Grzesiek, A. Bax, The origin and removal of artifacts in 3d HCACO spectra of proteins uniformly enriched with 13C, J. Magn. Reson. 102 (1993) 103–106.
[18] M. Piotto, V. Saudek, V. Sklenar, Gradient-tailored excitation for single quantum NMR spectroscopy of aqueous solutions, FEBS Lett. 2 (1992) 661–665.
[19] A.L. Davis, J. Keeler, E.D. Laue, D. Moskau, Experiments for recording pure absorption heteronuclear correlation spectra using pulsed field gradients, J. Magn. Reson. 98 (1992) 207–216.
[20] L.E. Kay, G.Y. Xu, A.U. Singer, D.R. Muhandiram, J.D. Forman-Kay, A gradient enhanced HCCH–TOCSY experiment for recording side chain 1H and 13C correlations in H_2O samples of proteins, J. Magn. Reson. 101 (1993) 333–337.
[21] A. Bax, D.G. Davis, MLEV-17 based 2D homonuclear magnetization transfer spectroscopy, J. Magn. Reson. 65 (1985) 355–360.
[22] R.A. Laskowski, J.A. Rullmannn, M.W. MacArthur, R. Kaptein, J.M. Thornton, AQUA and PROCHECK-NMR: programs for checking the quality of protein structures solved by NMR, J. Biomol. NMR 8 (1996) 477–486.
[23] R. Koradi, M. Billeter, K. Wuthrich, MOLMOL: a program for display and analysis of macromolecular structures, J. Mol. Graph. 14 (1996) 51–55.
[24] N.A. Farrow, R. Muhandiram, A.U. Singer, S.M. Pascal, C.M. Kay, G. Gish, S.E. Shoelson, T. Pawson, J.D. Forman-Kay, L.E. Kay, Backbone dynamics of a free and phosphopeptide-complexed Src homology 2 domain studied by 15N NMR relaxation, Biochemistry 33 (1994) 5984–6003.
[25] S. Grzesiek, A. Bax, The importance of not saturating HzO in protein NMR application to sensitivity enhancement and NOE measurements, J. Am. Chem. Soc. 115 (1993) 12593–12594.
[26] A. Barik, B. Mishra, L. Shen, H. Mohan, R.M. Kadam, S. Dutta, H.Y. Zhang, K.I. Priyadarsini, Evaluation of a new copper(II)–curcumin complex as superoxide dismutase mimic and its free radical reactions, Free Radic. Biol. Med. 39 (2005) 811–822.
[27] G.A. Wray, M.W. Hahn, E. Abouheif, J.P. Balhoff, M. Pizer, M.V. Rockman, L.A. Romano, The evolution of transcriptional regulation in eukaryotes, Mol. Biol. Evol. 20 (2003) 1377–1419.
[28] S. Smith, T. de Lange, TRF1, a mammalian telomeric protein, Trends Genet. 13 (1997) 21–26.
[29] D. Rhodes, L. Fairall, T. Simonsson, R. Court, L. Chapman, Telomere architecture, EMBO Rep. 3 (2002) 1139–1145.